

# Multipole Magnets with High Field Uniformity over Full Length for Super Separator Spectrometer

S. Manikonda, R. Meinke, J. Nolen, V. Prince and G. Stelzer

**Abstract**—First few nested superconducting multipole magnets to be used in the Super Separator Spectrometer ( $S^3$ ) device which is under construction at the GANIL laboratory in France have been manufactured and tested. The multipole magnets are based on a novel winding configuration for transverse magnetic fields of given multipole order, which closely approximates a pure cosine( $n\theta$ ) current density distributions over the entire length of the coil, including the coil ends. The windings are implemented as stacked saddle coils, a patented configuration, in which multiple conductor layers are inserted in precisely machined grooves. The resulting superconducting saddle coils achieve unprecedented magnetic field uniformity. In addition to highly suppressed systematic field errors, the resulting coils offer insignificant random field errors.

Multipole magnet measurements at room temperature and at of 4.2K have been performed. Tests have shown that the magnet meets the stringent magnetic field quality requirements and also that the magnet does not require any quench training which is unprecedented. We will present the novel coil design, practical implementation and discuss the performance of the magnets at final operating conditions.

**Index Terms**— Accelerator magnets, Superconducting coils, Superconducting magnets.

## I. INTRODUCTION

The Super Separator Spectrometer ( $S^3$ ) is a new device to pursue low energy nuclear physics research and is under construction at the GANIL laboratory in France [1] [2] [3]. The beam optics of  $S^3$  device requires twenty-four multipole magnets, of which twenty-one are superconducting multipole magnets. The remaining three operate in a radiation environment near the beam dump area and will not be discussed here. The Requirements for the  $S^3$  multipole magnets were developed to achieve large acceptance and high m/q resolution at final focal plane. And require multipole magnets with large apertures, short magnet length and high field uniformity over the full magnet length. Field

Automatically generated dates of receipt and acceptance will be placed here; authors do not produce these dates.

This work partially supported by the U.S. Department of Energy, Office of Science, Office of Nuclear Physics, under contract number DE-AC02-06CH11357 using resources of ANL's ATLAS facility, which is a DOE Office of Science User Facility.

S. Manikonda is with the AML Superconductivity and Magnetics, Palm Bay, FL 32905 USA (e-mail: [SManikonda@amls.com](mailto:SManikonda@amls.com)).

R. Meinke, is with AML Superconductivity and Magnetics, Palm Bay, FL 32905 USA (e-mail: [rbmeinke@amls.com](mailto:rbmeinke@amls.com)).

J. Nolen is with the Physics Division, Argonne National Laboratory, Lemont, IL 60439 USA (e-mail: [nolen@anl.gov](mailto:nolen@anl.gov)).

V. Prince, is with AML Superconductivity and Magnetics, Palm Bay, FL 32905 USA (e-mail: [VPrince@amls.com](mailto:VPrince@amls.com)).

G. Stelzer, is with AML Superconductivity and Magnetics, Palm Bay, FL 32905 USA (e-mail: [GStelzer@amls.com](mailto:GStelzer@amls.com)).

requirements for quadrupole, octupole and sextupole fields are summarized in Table 1. In addition dipole coils are used for vertical and horizontal steering corrections, requirements that are not stringent as compared to other multipoles and will not be discussed here. The usable magnet half aperture is 150 mm and is used as reference radius ( $R_{ref}$ ) for defining the field requirements. The most demanding coil of the required multipole magnet is the quadrupole coil, which operates at the largest current and requires the highest field.

Table 1: Magnetic field requirements for the  $S^3$  multipole magnets

	Quadrupole	Sextupole	Octupole
Half aperture (mm)	150	150	150
Field at reference radius (T)	1.2	0.4	0.2
Effective length (mm)	350	350	350
Error in gradient integral	<3%	<3%	<6%
Maximum skew harmonics	<0.1%	<0.1%	<0.1%

## II. SUPERCONDUCTING MULTIPOLE MAGNETS FOR $S^3$

AML Superconductivity and Magnetics Inc. is building the coils for the  $S^3$  superconducting magnets. Each superconducting multipole magnet or singlet consists of nested windings generating octupole, quadrupole, sextupole, and dipole fields. The twenty one singlets are grouped as seven Superconducting Multipole Triplets (SMT's) each housed in a single cryostat. The first few singlets have already been produced and tested at room temperature and cryogenic temperature. The first SMT is under assembly at Cryomagnetics, Inc. [4]. To our knowledge these are the first cosine-theta coils used in a nuclear physics spectrometer application. Below we present briefly the theory of constant cosine-theta coils.

### A. Constant Cosine- $m$ -Theta (CCmT) Coil Design Using Current Sheets

For a magnet with straight axis and rotationally symmetric magnetic field the multipole expansion of the radial magnetic field component is given by,

$$B_r(r, \theta, z) = \sum_{n=1}^{\infty} \left(\frac{r}{r_0}\right)^{n-1} (B_n(r, z) \sin(n\theta) + A_n(r, z) \cos(n\theta)),$$

where  $(r, \theta, z)$  are cylindrical coordinates,  $r_0$  is the reference radius,  $n$  is multipole order, and  $B_n(r, z)$  and  $A_n(r, z)$  are normal and skew components of the magnetic field. The skew term  $A_n(r, z)$  is zero for magnets with mid-plane symmetry and is neglected in the present discussion. For an infinitely long cylindrical coil with current flowing in axial direction ( $z$ ) a current density  $J_z = j_0 \cdot \cos(m\theta)$  generates a pure normal multipole field of order  $m$ , where  $m = 1$  gives a dipole field,  $m = 2$  a quadrupole field etc. A cosine( $m\theta$ ) current density distribution can be achieved by either using current sheets

with  $\cos(m\theta)$  current density variation, or by current blocks with constant current, but optimized block geometry [4]. A Coil design based on the current sheet approach was used for the  $S^3$  multipole magnet coils. It is possible to approximate current sheets on cylinders by a discrete set of wires, whose angular positions are given by solving the equation,  $\sin(m\theta) = (i - 1/2)/N$ , where  $m$  determines the multipole order,  $\theta$  gives the angular positions of the wires,  $i$  is the individual wire number, and  $N$  is the total number of wires. A system of nested coils can be used for a combined function magnet, using individual current sheets for each required multipole order.

For finite length cosine-theta coils, in particular with small aspect ratios of length to diameter, as is the case for the  $S^3$  magnets, the contribution of the coil ends to the integrated field is of utmost importance. A saddle coil with ends based on stream functions, a widely used technique in MRI gradient coil design [5], was proposed by P. Walstrom to produce a perfect  $\cos(m\theta)$ -field in the central part as well as in the end-field region of accelerator magnets [6] [7] [8]. This approach approximates the ideal  $\cos(m\theta)$  current density distribution locally at every position along the coil axis including the coil ends. Using this approach, the conductor layout in the coil ends is determined by solving the implicit equation,  $f(z) \cdot \sin(m\theta) = (n - 1/2)/N$ , where the function,  $f(z) \cdot \sin(m\theta)$ , is called the stream function, and  $f(z)$  is a shape function that describes the shape of the coil ends. For some special choices of the shape function the above equation can be solved explicitly. For example the shape function,  $f(z) = \cos(\pi \cdot (z - L_s/2)/(2 \cdot L_E))$ , is used for the  $S^3$  magnets, where  $L_s$  is tip-to-tip length of the magnet, and  $L_E$  is the length of the coil end region. The resulting coil pattern generated for the octupole coil can be seen in Figure 4.

### B. Implementation of CCmT Coil for the $S^3$ magnets

Perfect CCmT coils comprised of an infinite number of discrete current loops is not possible for practical implementation. A novel winding configuration based on finite number of turns which closely approximates an ideal cosine-theta coil and includes turn to turn transitions, layer to layer transitions, subcoil to subcoil transition, and connection to current leads was developed. Such windings can accommodate minimum bend radius requirements for a superconductor, spacing necessary for machining and placing wires, and other application specific requirements. Winding is implemented as stacked saddle coils, a patented configuration [9] [10], in which multiple conductor layers are inserted in precisely machined grooves. All deviations from an ideal CCmT coil will impact field quality. A comparison of field quality for the  $S^3$  quadrupole coil based of different coil designs is shown in Figure 1. It shows unprecedented magnetic field uniformity can be achieved with CCmT coils.

### C. $S^3$ coil design

The nested windings are implemented as four concentric CCmT type coils would on a mandrel. The superconducting multiplets are 450 mm long and the warm-bore diameter is 336 mm. The dipole correction coils are the outermost of the nested coils, with the sextupoles, qadrupole and the octupoles

at successively smaller radii. Placement of wires is shown in the singlet cross-section view in Figure 2.

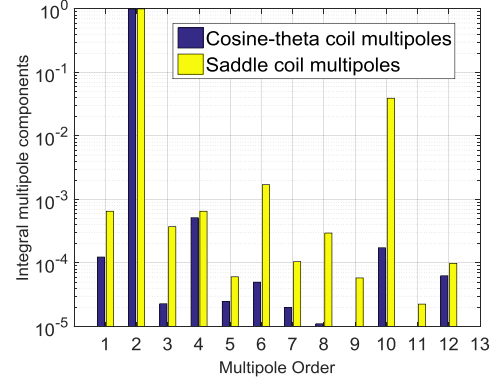


Figure 1: Comparison of integral multipole content for a realistic cosine-theta quadrupole with a realistic saddle coil.

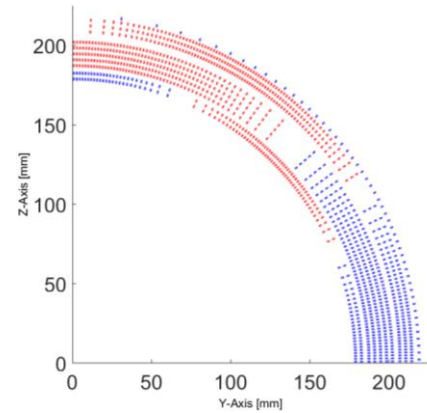


Figure 2: Cross section view at the center of the magnet showing singlet wire placement in one quadrant. Starting from inside two double layers for octupole, five double layers for quadrupole, three double for sextupole and one double layer for dipole coil are shown. The red and blue colors represent the direction of currents.

### D. Iron yoke around the singlet

To reduce transfer function non-linearity and reduce warm-up and cool down times of the magnets, a magnet design with room temperature iron yoke is used. The iron yoke, made from steel 1010, has an inner radius of 337 mm, 50 mm thick and 350 mm long and is placed symmetrically around the singlet. Computed deviation in field linearity is less than 0.05 %. Iron outside also helps in clamping the stray transverse field.

### E. Field quality and coil optimization

Field quality is defined by integral quantities along a line parallel to central axis covering the fringe field region,  $\pm 1$  m. For a magnet with main multipole of order  $m$ :

- **Integral field error** is defined as the error in the multipole field at reference radius relative to main multipole field.
- **Relative deviation in integral field gradient** is defined as deviation of integral field gradient of order  $m$  with respect to radial position computed at reference radius relative to corresponding integral along the central axis.

- **Effective length** is defined as the length required, assuming there is no coil ends, to give same integrated field strength for the main multipole field.

AML's proprietary CoilCAD toolbox [12] was used to design, optimize and generate CNC machine code for the superconducting  $S^3$  coils.

#### F. Choice of conductor and operating margin

The developed superconducting coil design is based on 0.8 mm diameter NbTi superconductor, specifications and performance of the conductor for  $S^3$  operating conditions are summarized in Table 3.

Table 2: Table summarizing main magnet design parameters. Dipole parameters are not shown.

	Octupole	Quadrupole	Sextupole
<b>Coil Design Parameters</b>			
Number of double layers	2	5	3
Number of turns per layer	25	52	38
Coil inner diameter (mm)	356.10	372.11	416.11
Coil outer diameter (mm)	368.10	410.11	436.11
Straight section length (mm)	290	225	235
Minimum bend radius (mm)	5.45	7.04	7.33
Layer spacing (mm)	1	1	1
Conductor length (m)	683	1697	1218
Coil Inductance (mH)	28	400	110
<b>Field Parameters from CoilCAD simulations</b>			
Maximum coil current (A)	260	465	365
Field at reference radius (T)	0.21	1.34	0.39
Relative error in gradient integral (%)	0.14	0.07	0.05
maximum skew error (%)	0.03	0.03	0.03
maximum self-field in coil with iron (T)	0.45	2.06	1.00
Field enhancement due to iron yoke (%)	<1	7	5.2
<b>Quench Protection Parameters</b>			
Maximum stored energy (kJ)	1.00	46.70	7.12
Dump resistor type	External	Internal	External
Dump resistor value ( $\Omega$ )	0.5	0.7 @ 4.2 K	0.750
Peak voltage (V)	130	600	270
Peak temperature (K)	40	100	100
Maximum ramp rate (A/s)	250	5	60

Table 3: NbTi superconductor specifications and performance at final operating condition of  $S^3$

	Units	
<b>NbTi conductor specifications</b>		
Number of strands		1
NbTi wire diameter	mm	0.80
Formvar insulation thickness	mm	0.05
Number of NbTi filaments		4158
Cu RRR		100
n-value of NbTi superconductor		30
Copper to non-copper ratio		1.6
Critical current density @ 4.2 K & 5 T	A/mm <sup>2</sup>	2900
<b>Performance of the conductor</b>		
Nominal temperature	K	4.35
Critical temperature	K	5.37
Nominal current	A	465
Critical current	A	666
Assumed Peak field at nominal current	T	4
Current margin	%	43
Temperature margin	K	1

#### G. Manufacturing of Singlets

##### 1) Coil Support Structure

The CCmT coil windings are embedded in fiber-reinforced composite structures and are built around a central stainless steel (SS) bobbin on the inside, which also serves as the helium containment vessel. On the outside the coils are surrounded by aluminum rings that put the coil under pre-stress at the operational temperature, as shown in Figure 3. A slip plane introduced between the coil pack and the SS bobbin eliminates thermal stress development during cool down.



Figure 3: Picture on the left show manufactured singlet with aluminum containment ring. Picture on the right shows the cryostat housing the three singlets



Figure 4: Coil support cylinder with machined grooves for a SSC CCmT coil. Grooves in lighter shade already have conductors placed in them.

##### 1) Coil Manufacturing

A stacked saddle coil (SSC) configuration comprising of two layers placed in a groove was chosen for  $S^3$  multipole coils. With a proprietary process the conductors are stabilized in the grooves, which prevents any conductor movement under the influence of acting Lorentz forces, when the coil is excited [10] [9]. The conductor support grooves are machined on computer-controlled machining centers achieving high accuracy in conductor placement thereby limiting random field errors. The SSC arrangement offers the additional advantage of increasing transverse quench propagation velocity, since the conductors of two coil layers are in close contact without additional material with high thermal resistivity in between. A SSC octupole double layer with NbTi superconductor placed in grooves is shown in Figure 4.

#### H. Quench Protection and Detection

The development of a quench is detected by a conventional quench detection system using voltage taps, and the power

supply driving the transport current in all superconducting coils of an SMT are disconnected in about 10 ms. In case of quench, protection for octupole and sextupole coils is based on external dump resistors. The parameters for protection system are given in Table 2. Due to a relatively large stored energy of about 46 kJ in the quadrupole coil at nominal current, its quench protection is more challenging. Computations have shown that 30% of the stored energy is absorbed in inner steel bobbin and outer aluminum rings, containment for the coil pack, during the quench. A novel quench protection system that consists of an internal dump resistor made of specially chosen copper alloy, with a residual-resistivity ratio (RRR) of  $\sim 9$ , was developed. This internal dump resistor consists of a low inductance bifilar coil, which is located between first two super layers of the quadrupole coil and is electrically in parallel to the whole quadrupole. During a quench the normal conducting winding of the dump resistor heats up and spreads the quench over a large area of the superconducting winding mitigating the peak temperature. With rising temperature resistance increases, thereby further increasing the effectiveness of the dump resistor. The specific choice of RRR for the bifilar coil limits the peak temperature in the coil to 100 K and peak voltage across the dump resistor during quench to 600 V.

### I. $S^3$ superconducting multipole triplet assembly

$S^3$  singlets are arranged as triplets in their cryostats, for a total of 12 set of coils powered by 8 single quadrant power supplies. A view of the manufactured cryostat can be seen in Figure 3. Neighboring singlets in the triplet are separated by 86 mm drift space. There are eight multipole triplets in  $S^3$ , of which seven are superconducting and one is a room-temperature open triplet placed before the beam dump image. The three quadrupole coils of each triplet will always operate with alternate polarity and can be configured to use only four current leads by using two common current leads. This also reduces the heat load on the two common-mode leads. The same configuration applies to set of three sextupoles and three octupoles.

### III. TESTING OF SINGLETS

A cryogenic test of the first few singlets was performed to establish performance under final operating conditions. The cold measurements are based on harmonic coils technique [12]. It is worth noting that no quench training was required to operate these coils, which to our knowledge is unprecedented for such magnets. Figure 5 shows very good agreement achieved between the experimentally measured and the CoilCAD simulation of the quadrupole field at maximum current of 500 A used during testing. Figure 6 shows the hysteresis of first two allowed terms of the quadrupole field, normal components B6 and B10, during the ramp up and ramp down cycle. Figure 7 shows the experimentally measured quadrupole field error at reference radius measured as a function of excitation current during the ramp up and ramp down cycle. Even at low excitation current, where persistent currents can impact the field quality, the field quality achieved is better than the specified by the  $S^3$  requirements. Room temperature testing and qualification of multipole coils is also

performed after manufacturing of each singlet. Detailed discussion cold and warm measurement procedure, analysis and results will be part of separate publication.

### IV. CONCLUSION

Unprecedented field uniformity is achieved over almost the complete coil aperture of  $S^3$  multipole magnets using patented CCmT SSC winding configurations. The approach significantly reduced size, weight, cryogenic system requirements and cost of the superconducting magnets. The coils operate without any quench training.

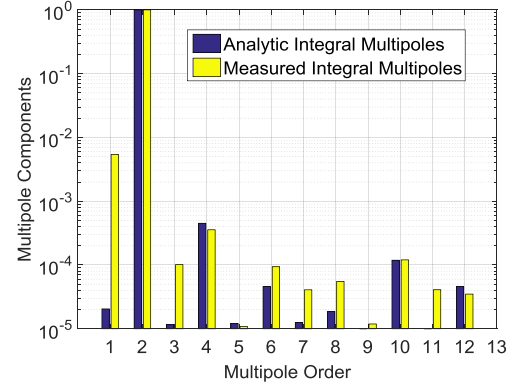


Figure 5: Comparison of experimentally measured and computed integral multipoles fields for quadrupole at 500 A and at reference radius. Field are normalized to the main pole, quadrupole.

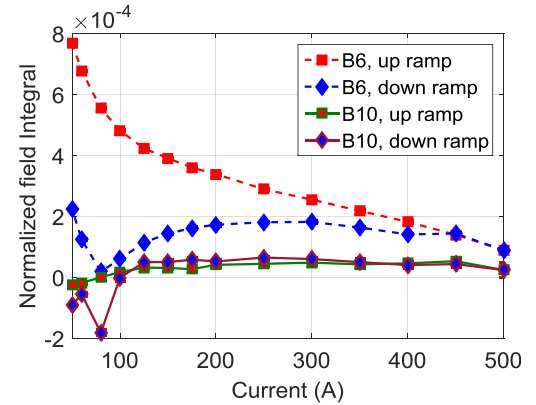


Figure 6: Hysteresis of first two allowed terms of the quadrupole, B6 and B10. Total of 632 uncompensated and compensated measurement were performed for analysis covering 36 current settings

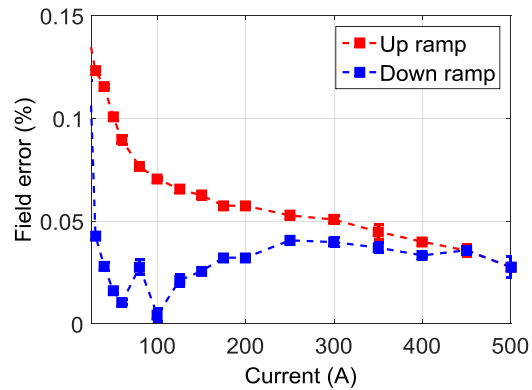


Figure 7: Experimentally measured quadrupole field error at reference radius measured as a function of excitation current

## REFERENCES

- [1] F. Dechery, A. Drouart, H. Savajols, J. Nolen, M. Authier, A. Amthor, D. Boutin, O. Delferriere, B. Gall, A. Hue, B. Laune, F. Le Blanc, S. Manikonda, J. Payet, M.-H. Stodel, E. Traykov and D. Uriot, "Toward the drip lines and the superheavy island of stability with the Super Separator Spectrometer S3," *The European Physical Journal A*, vol. 51, no. 6, 2015.
- [2] A. Drouart, A. Amthor, D. Boutin, O. Delferrière, M. Duval, S. Manikonda, J. Nolen, J. Payet, H. Savajols, M.-H. Stodel and D. Uriot, "The Super Separator Spectrometer (S3) for SPIRAL2 stable beams," *Nuclear Physics A*, vol. 834, no. 1-4, pp. 747c - 750c, 2010.
- [3] A. Drouart, B. Erdelyi, B. Jacquot, S. Manikonda, J. Nolen, H. Savajols and A. Villari, "Design study of a pre-separator for the LINAG super separator spectrometer," *Nuclear Instruments and Methods in Physics Research Section B: Beam Interactions with Materials and Atoms*, vol. 266, no. 19-20, pp. 4162-4166, 2008.
- [4] "Superconducting Magnet Manufacturer - Cryomagnetics, inc.," [Online]. Available: <http://www.cryomagnetics.com/>.
- [5] R. A. Beth, "Elliptical and Circular Current Sheets to Produce a Prescribed Internal Field," *Nuclear Science, IEEE Transactions on*, vol. 14, no. 3, pp. 386-388, June 1967.
- [6] R. Turner, "Gradient coil design: a review of methods," *Magnetic Resonance Imaging*, vol. 11, no. 7, pp. 903-920, 1993.
- [7] P. Walstrom, "Design of End Turns in Current-dominated Dipole and Quadrupole Magnets for Fields with Low Higher Harmonic Content," in *European Particle Accelerator Conference*, 2002.
- [8] P. Walstrom, "Soft-edged magnet models for higher-order beam-optics map codes," *Nuclear Instruments and Methods in Physics Research Section A: Accelerators, Spectrometers, Detectors and Associated Equipment*, vol. 519, no. 1-2, pp. 216-221, 2004.
- [9] P. L. Walstrom, "Magnetic Fields and Inductances of Cylindrical Current Sheet Magnets," 1990.
- [10] R. Meinke, *Methods of fabricating a conductor assembly having a curvilinear arcuate shape*, Google Patents, 2011.
- [11] R. Meinke and G. Stelzer, "Wiring assembly and method of forming a channel in a wiring assembly for receiving conductor". United States of America Patent 7,864,019, 2011.
- [12] "Perfect-Field™ Process | AML Superconductivity and Magnetics," [Online]. Available: <http://amlsuperconductivity.com/capabilities/perfect-field-process/>.
- [13] A. K. Jain, "Measurements of field quality using harmonic coils," *US Particle Accelerator School on Superconducting Accelerator Magnets*, 2001.
- [14] S. Kim, "Tagential winding coil probes for dipole, quadrupole and sextupole magnet measurements," 1995.
- [15] L. Walckiers, "The harmonic-coil method, parts 1 and 2," 1992.